

GASFLOW simulations for cryogenic tank loss of vacuum scenarios

用 GASFLOW 模拟真空环境下低温罐损失

J.R. Travis¹ and D. Piccioni Koch^{2*}

¹ Engineering & Scientific Software, Inc., 2128 S. Ensenada Circle, Rio Rancho, NM 87124, USA

² Steinbuch Centre for Computing (SCC), Karlsruhe Institute of Technology (KIT), Postfach 3640, 76021 Karlsruhe, Germany

daniela.piccioni@kit.edu

Accepted for publication on 27th February 2015

Abstract - The Computational Fluid Dynamic (CFD) code GASFLOW was used to simulate Loss of Vacuum scenarios for studying the safety performance of high-pressure hydrogen vessels for vehicular storage applications. For these simulations, the real gas equations of state (EoS) for hydrogen based on the Leachman's NIST reference model and a modified van der Waals model were used. The GASFLOW simulations show good agreement with previous simulation results and with data.

Keywords – Computational Fluid Dynamic Code, Real Gas Equations of State for Hydrogen, High-pressure Hydrogen Vessel Loss of Vacuum, Hydrogen Energy.

I. INTRODUCTION

Hydrogen represents one of the most favorable gases as a future alternative energy source. However, in the automotive field, several challenges must be overcome before the introduction of hydrogen fuel cell vehicles on a large scale can become possible. One key hurdle is the development of efficient and safe hydrogen storage technologies and, in particular, the realization of high-pressure hydrogen vessels for long term viability.

The Computational Fluid Dynamic (CFD) code GASFLOW [1, 2, 3] was used to simulate Loss of Vacuum scenarios for studying the safety performance of high-pressure hydrogen vessels for vehicular storage applications. The simulations presented in this paper were carried out in the frame of the “CryoSys” project [4], whose partners were the Bayerische Motoren Werke (BMW) Group, the Karlsruhe Institute of Technology (KIT), AIRBUS Operations and ET Energie Technologie. The main aim of this project was the development of Cryo-compressed Hydrogen (CCH₂) vessels for automotive applications (CryoSys vessels) and, in particular, the realization of Al-liner carbon-fiber/epoxy tanks of Type III [5]. GASFLOW has been extended to include real

gas equations of state (EoS) for hydrogen [6,7]. These EoS options include Leachman's NIST reference model [8, 9] and a modified van der Waals model [6,7].

Three simulations are presented in this paper as Loss of Vacuum representative:

1. For a reference case, the outer steel shell of the vessel is removed and the Carbon-Fiber-Epoxy (CFE) surface is directly exposed to ambient air;
2. The outer shell is intact, but there is outside loss of vacuum with the ambient air leaking into the annulus; and
3. The outer shell is intact, but there is inside loss of vacuum with hydrogen leaking from the tank into the annulus.

An exact solution for constant volume heating can be found for various initial conditions. Another exact solution for an ideal discharge, the isentropic solutions, can be found for the cryogenic tank blowdown into the vacuum volume. The time required to achieve the equilibrium state is simulated and presented.

All heating solutions require a temperature-dependent natural convective heat transfer coefficient model to account for the outer surface, either CFE or outer Aluminum shell, boundary condition; this accounts for the cryogenic tank cylindrical geometry interacting with ambient air conditions at 1 atmosphere and 300 K. This model has been implemented into GASFLOW and is described in detail in this paper.

The GASFLOW simulations show good agreement with previous simulation results and with data.

II. AN EXACT SOLUTION HEATING MODEL

The idea behind the exact heating solution is that in a loss of vacuum situation, the insulation of the tank is no longer functioning because ambient air leaks in the vacuum space. In

time, no matter what the heat transfer, the tank will warm to the ambient temperature (300 K) and the pressure in the tank will be as the exact heating model solution shows. Leachman's

NIST hydrogen equation of state [8, 9] can be used to compute an exact solution for constant volume heating. We present the solution in the following manner:

1. Select an initial temperature; for example, 40 K.
2. Select a range of initial pressures; for example, 2.5 MPa to 25 MPa in increments of 2.5 MPa.
3. Compute the hydrogen densities for the selected initial temperature and each pressure value by inverting the NIST pressure equation

$$p = p(\rho, T). \quad (1)$$

4. Select a final temperature; for example, 300 K, or select a final pressure; for example 40.2 MPa (when the mechanical safety vent opens [10]).

5. Compute the final pressure using the selected final temperature or compute the final temperature using the selected final pressure and the hydrogen densities found in step 3.

We have plotted this exact heating solution in Figures 1 and 2.

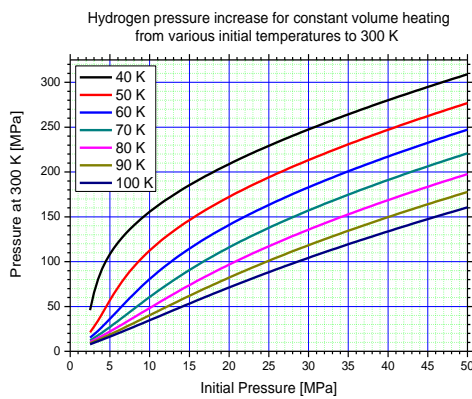


Figure 1. An exact pressure solution for hydrogen constant volume heating from a given initial temperature and pressure to the final temperature at 300 K.

An example can be demonstrated by selecting an initial pressure 30 MPa and temperature 65 K, and then reading from Figure 1, we see the final pressure is roughly 170 MPa (actually 169.46 MPa).

Perhaps a more relevant representation of this exact heating solution is to select the final pressure based on the opening of the mechanical safety vent at 40.2 MPa \pm 3% [10]. Figure 2 gives this result.

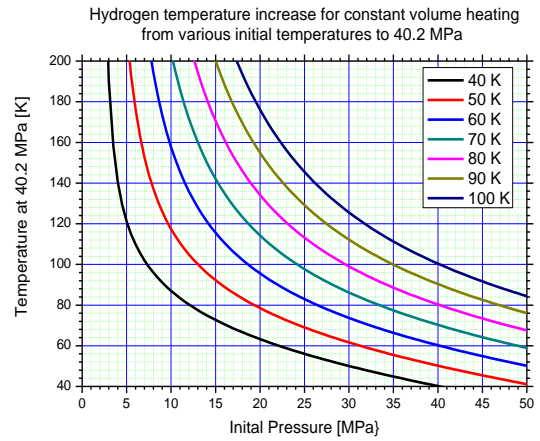


Figure 2. An exact temperature solution for hydrogen constant volume heating from a given initial temperature and pressure to the final pressure at 40.2 MPa.

The same example as before (initial conditions: 30 MPa and 65 K) shows that heating the CryoSys Tank from 65 K to 80 K increases the pressure to 40.2 MPa where the mechanical safety vent opens to protect the integrity of the tanks.

III. GASFLOW CRYOSYS TANK GEOMETRIC MODEL, INITIAL CONDITIONS, AND BOUNDARY CONDITIONS

The GASFLOW geometric model is a right-circular cylinder. The inner diameter is 279 mm and the length is 1872.87 mm yielding a free volume of 114.5 liters. The interior structures have been removed for simplicity. The mesh consists of 3 radial cells, 13 azimuthal cells, and 52 axial cells for a total of 2,028 cells. As a mesh convergence test, we doubled the number of cells in each coordinate (6 radial, 26 azimuthal, 104 axial: totally 16,224 cells without significant differences between the coarse and medium mesh representation.

For all reported simulations, the initial conditions inside the tank are: pressure 30 MPa, temperature 65 K, and density 66.253 kg/m³.

The boundary conditions are as follows:

1. For the case where the outer steel shell is removed, the tank wall is a composite structure with 4.0 mm aluminum and 9.5 mm carbon-fiber epoxy.
2. For the case where the outer aluminum shell is intact but the annulus is filled with air to a volume equaling 40 liters (outside loss of vacuum) in less than 1 minute [10], the gap width is 15mm with a 4 mm outer aluminum shell.
3. For the case where the Aluminum shell is intact but the annulus is filled from the inside with hydrogen to a volume equaling 40 liters (inside loss of vacuum) through an orifice with a diameter of 0.18 mm [10].

In all cases, the outermost structural surface (CFE or Aluminum) is coupled to the ambient (0.101325 MPa and 300 K) with the natural convective heat transfer coefficient described below.

The first two cases, the reference bare CFE tank and the outside loss of vacuum, are straight forward simulations, while the inside loss of vacuum case is extremely complex. In the next section, we will focus our attention to the inside loss of vacuum scenario, and then return to the reference bare CFE tank and outside loss of vacuum in section V.

IV. INSIDE LOSS OF VACUUM

A. The Isentropic Scenario

As mentioned above, the CryoSys Tank, 114.5 liter volume, is initially at 30 MPa, 65 K, and 66.253 kg/m³, which gives an initial mass equaling 7.586 kg. Should one open an exit hole (assumed to be an orifice with a 0.18 mm diameter [10]), an isentropic expansion into the vacuum gap, 40 liter volume, would result in pressure equilibrium with average density equaling 49.1 kg/m³. Since the process is isentropic, one can readily find the exact final thermodynamic state for both tank and vacuum gap as 43.049 K and 5.6754 MPa. Table 1 provides a quick summary of the initial and final states.

Table 1. Summary of the Exact Isentropic Inside Loss of Vacuum Solution.

| CryoSys Tank | Vacuum Volume | Total Volume |
|---|--|--|
| 0.1145 m ³ | 0.040 m ³ | 0.1545 m ³ |
| P = 30 MPa T = 65 K $\rho = 66.253$ kg/m ³ | P = 0 MPa T = 0 K $\rho = 0$ kg/m ³ | P = 5.6754 MPa T = 43.049 K $\rho = 49.10$ kg/m ³ |

Figure 3 provides a simple schematic of the physical processes, namely the discharge or blowdown of the CryoSys Tank into the vacuum volume, while the T-S diagram in Figure 4 shows the stated processes: initial condition in the CryoSys Tank labeled “A”. initial condition in the vacuum volume labeled “E”, and the final or equilibrium condition labeled “B”.

The CryoSys Tank discharge and the vacuum volume filling are as follows:

A → B is the discharge path taken in the CryoSys Tank.

E → D shows that initially the discharge expansion into the vacuum volume results in temperatures and pressures less than the triple point, which would produce solid hydrogen.

D → C shows that as the vacuum volume filling continues a two-phase mixture of liquid and vapor occupies this volume. Figure 5 shows the quality and pressure as a function of temperature during this process. Note that near “D” a three-phase mixture can occur.

C → B is the vacuum volume vapor condition as the final equilibrium state is approached.

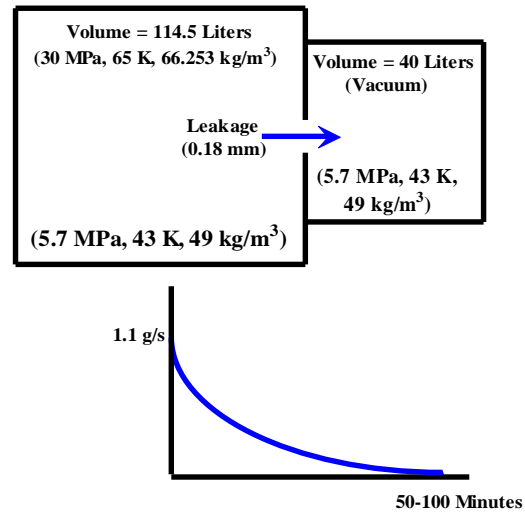


Figure 3. Schematic diagram illustrating the Inside Loss of Vacuum scenario.

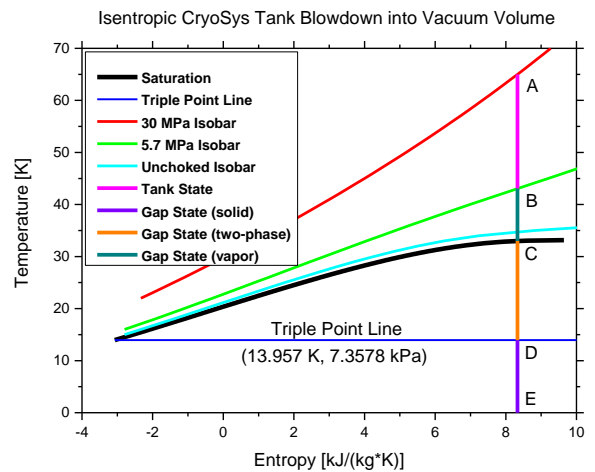


Figure 4. T-S diagram showing the Inside Loss of Vacuum thermodynamic paths.

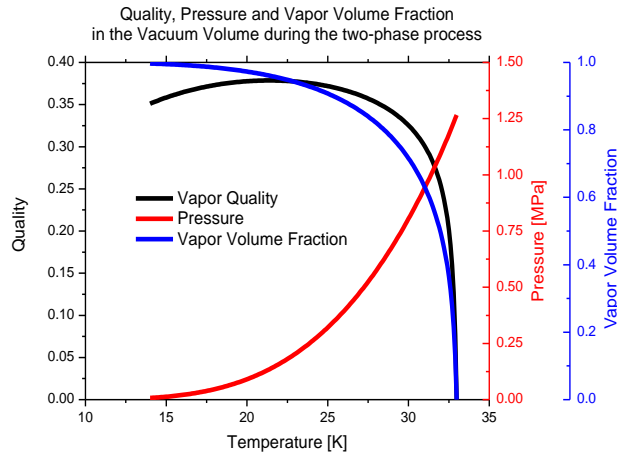


Figure 5. Quality, Pressure and Vapor Volume Fraction in the Vacuum Volume during the two-phase process (D → C in Figure 4).

As the CryoSys Tank discharges, the flow is at first choked and then unchokes as will be seen later in this analysis. For references purposes, the unchoked isobar condition is presented in Figure 6. This means a choked discharge exists until the choked pressure decreases to the pressure in the vacuum volume, the unchoked isobar (1.77 MPa at 34.758 K), at which time the discharge becomes unchoked. It is clear that the discharge remains single phase at the discharge orifice and after unchoking the conditions in both volumes are single-phase.

We know the involved thermodynamic states, so what remains to find is the time to achieve these states. This requires determining the solution for the following system of equations for the conservation of mass and energy:

$$\frac{d}{dt}(\rho_T V_T) = -C_d \dot{m}_t \quad (2)$$

$$\frac{d}{dt}(\rho_T I_T V_T) = -C_d \dot{m}_t \left(h + \frac{V^2}{2} \right)_t \quad (3)$$

$$\frac{d}{dt}(\rho_{VV} V_{VV}) = C_d \dot{m}_t \quad (4)$$

$$\frac{d}{dt}(\rho_{VV} I_{VV} V_{VV}) = C_d \dot{m}_t \left(h + \frac{V^2}{2} \right)_t \quad (5)$$

During the discharge initial phase when the flow is choked, one can determine the choked or critical mass flow rate, \dot{m}_t , by solving the coupled equations [11]

$$s(T_T, \rho_T) = s(T_t, \rho_t) \quad (6)$$

$$2[h(T_T, \rho_T) - h(T_t, \rho_t)] = w(T_t, \rho_t)^2, \quad (7)$$

for the choked temperature, T_t , and density, ρ_t , and knowing the tank temperature, T_T , and density, ρ_T , gives the choked mass flow rate as

$$\dot{m}_t = \rho_t \cdot A \cdot w(T_t, \rho_t). \quad (8)$$

When the choke pressure, $p(T_t, \rho_t)$, is less than the vacuum volume pressure, $p(T_{VV}, \rho_{VV})$, the flow unchokes and the discharge velocity is found from

$$w(T_t, \rho_t) = \sqrt{2[h(T_t, \rho_t) - h(T_{VV}, \rho_{VV})]}, \quad (9)$$

where the unchoked mass flow rate is

$$\dot{m}_t = \rho_{VV} \cdot A \cdot w(T_t, \rho_t). \quad (10)$$

For the following solution of Equations (2-10), the discharge coefficient, C_d , is unity. In Figure 6 the time-dependent pressure is given for the CryoSys Tank, Vacuum Volume, and choked (unchoked) orifice pressure. Note that the flow becomes unchoked when the orifice pressure is less than the Vacuum Volume pressure. This occurs at approximately 2100 s.

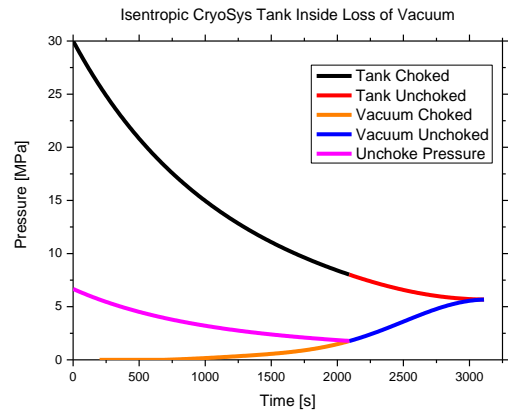


Figure 6. Time-dependent pressures for the isentropic Inside Loss of Vacuum solution of Equations (2-10).

In Figures 7-9, the densities, temperatures, and discharge mass flux are presented, respectively, for the isentropic Inside Loss of Vacuum solution of Equations (2-10).

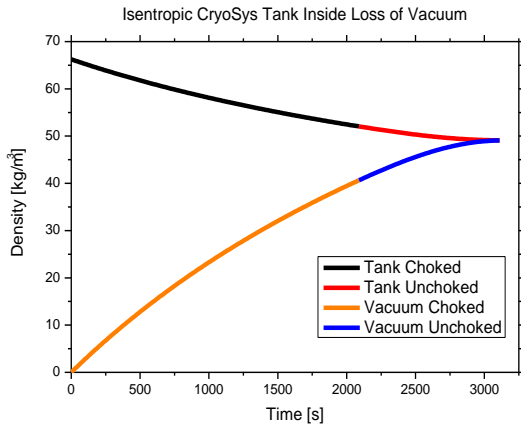


Figure 7. Time-dependent densities for the isentropic Inside Loss of Vacuum solution of Equations (2-10).

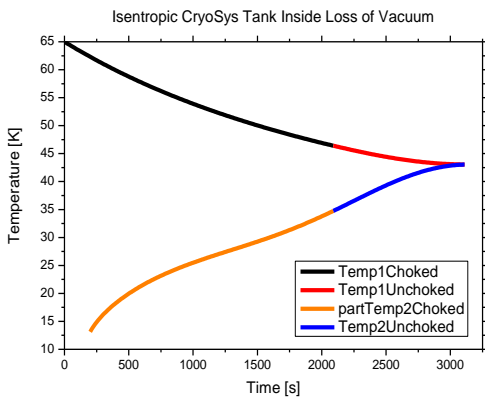


Figure 8. Time-dependent temperatures for the isentropic Inside Loss of Vacuum solution of Equations (2-10).

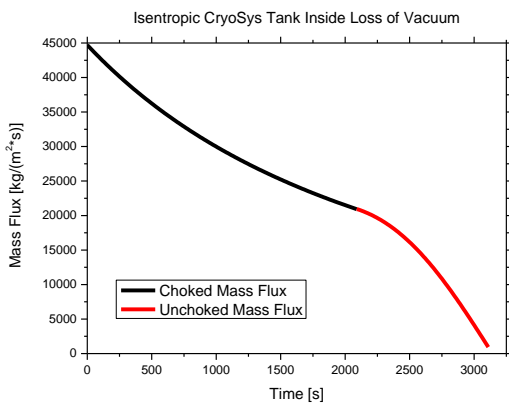


Figure 9. Time-dependent mass flux for the isentropic Inside Loss of Vacuum solution of Equations (2-10).

Observe that the final state is reached in about 3200 s with final state values identical to those given in Table 1. One can see from Figure 8 the timings for each of the vacuum volume processes given in Figure 4. We summarize these timings in Table 2.

TABLE 2. TABULATION OF THE VACUUM VOLUME PROCESSES SHOWN IN THE T-S DIAGRAM (FIGURE 4) AND OBSERVED IN FIGURE 8.

| Vacuum Volume processes shown in Figure 4 | Observed time from Figure 8 (seconds) |
|---|---------------------------------------|
| E → D: Solid-phase | 200 |
| D → C: Two-phase | 1675 |
| C → B: Single-phase | 1325 |
| TOTAL | 3200 |

B. The External Heat Transfer Scenario

In actuality, as the blowdown from the CryoSys Tank into the vacuum volume occurs, there is heat transferred to the outer Aluminum shell by natural convection from the ambient conditions (1 atmosphere at 300 K).

Hydrogen thermal conductivity will play a major role during the CryoSys heating. Using the serial mixing rule for multiphase mixtures, we construct a typical hydrogen temperature-dependent thermal conductivity in Figure 10 by using the discharge results presented above.

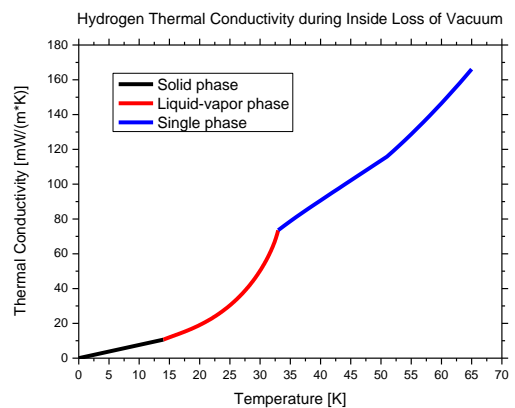


Figure 10. A typical Hydrogen temperature-dependent thermal conductivity behavior for the multiphase processes for the isentropic discharge scenario shown above.

Following the work of Spang [12], the average Nusselt Number for a horizontal cylinder is given by

$$Nu(T_m) = \frac{h \cdot D}{k(T_m)} = \left\{ \sqrt{Nu_0} + \left[\frac{Gr(T_m) \cdot Pr(T_m)}{300} \right]^{\frac{1}{6}} \right\}^2 ; Nu_0 = 0.36 , \quad (11)$$

$$\left[1 + \left(\frac{0.5}{Pr(T_m)} \right)^{\frac{9}{16}} \right]^{\frac{16}{9}}$$

where the Grashof Number is

$$Gr(T_m) = \frac{D^3 \cdot g \cdot \rho(T_m)^2 \cdot \beta(T_m) \cdot |T_{surf} - T_{amb}|}{\mu(T_m)^2} , \quad (12)$$

the Prandtl Number is

$$Pr(T_m) = \frac{\mu(T_m) \cdot c_p(T_m)}{k(T_m)} , \quad (13)$$

where all fluid properties are evaluated at the mean temperature

$$T_m = \frac{1}{2} (T_{surf} + T_{amb}) . \quad (14)$$

Correlation (Equation 11) is judged to be valid for

$$10^{-4} \leq Gr \cdot Pr \leq 4 \cdot 10^{14} \quad \text{and} \quad 0.022 \leq Pr \leq 7640 .$$

The air properties at 101.325 kPa are required to compute the time-dependent heat transfer coefficient between the CFE or steel shell surface and ambient conditions. These time-dependent properties are taken from Kays and Crawford [13]. Least Squares approximations have been found and are also shown in the following three Figures (11-13).

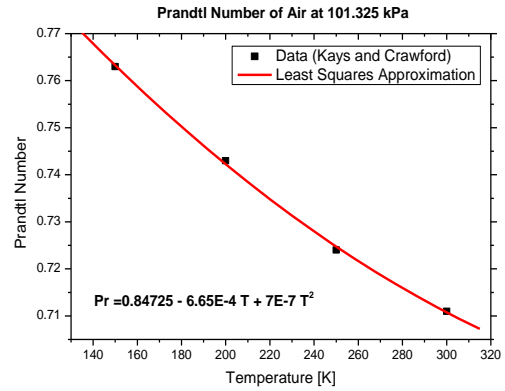


Figure 11. Air Prandtl Number as a Function of Temperature at 101.325 kPa.

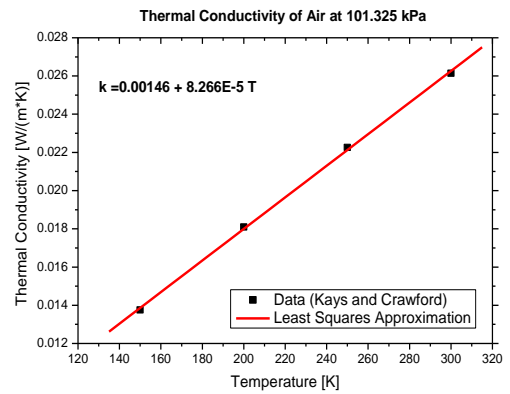


Figure 12. Air Thermal Conductivity as a Function of Temperature at 101.325 kPa.

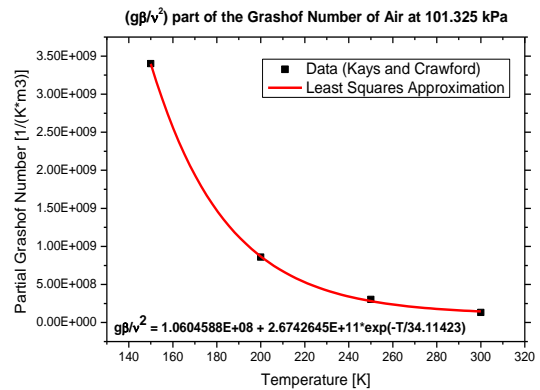


Figure 13. Air Partial Grashof Number as a Function of Temperature at 101.325 kPa.

A heat flow energy balance for a cylindrical system from the ambient conditions to the inside of the CryoSys Tank can be constructed as

$$q = \frac{2\pi L(T_{\infty} - T_{inside})}{\frac{1}{r_1 h_{inside}} + \frac{\ln(r_2/r_1)}{k_{Al}(T)} + \frac{\ln(r_3/r_2)}{k_{CFE}(T)} + \frac{\ln(r_4/r_3)}{k_{MII}(T)} + \frac{\ln(r_5/r_4)}{k_{Al}(T)} + \frac{1}{r_5 h_{outside}}} \quad (15)$$

where the temperature-dependent thermal conductivities are given in Figures 14-16 and the outside heat transfer coefficient, $h_{outside}$, is computed from Equation (11). Table 3 summarizes the geometry given in Equation (15).

TABLE 3. GEOMETRY DESCRIPTION GIVEN IN EQUATION (15)

| Radial Position | Distance (m) | Description |
|-----------------|--------------|---|
| r1 | 0.1395 | Inner CryoSys Tank $\leq r1$ |
| r2 | 0.1435 | $r1 \leq$ inner Al shell \leq $r2$ |
| r3 | 0.153 | $r2 \leq$ CFE \leq $r3$ |
| r4 | 0.168 | $r3 \leq$ MII \leq $r4$ |
| r5 | 0.172 | $r4 \leq$ outer Al shell \leq $r5$ |
| | | Ambient $\geq r5$ |

With nearly stagnation conditions in the CryoSys tank, the inside heat transfer coefficient, h_{inside} , can be approximated by $h_{inside} = k_{H2}/r_1$, where the single phase hydrogen thermal conductivity can be found as a function of pressure and temperature from Figure 17.

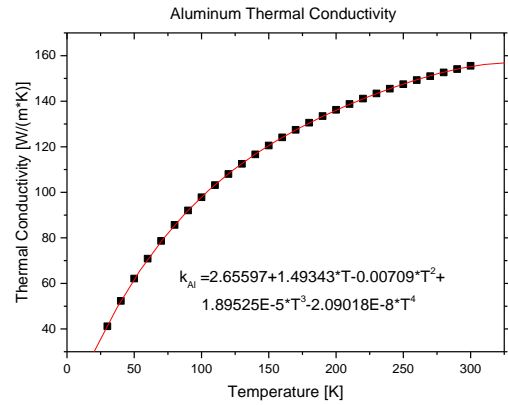


Figure 14. Aluminum thermal conductivity as a function of temperature.

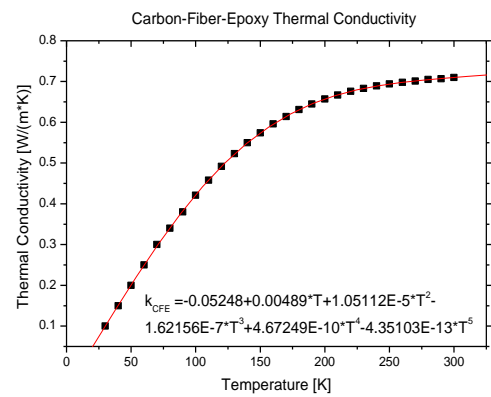


Figure 15. Carbon-Fiber-Epoxy thermal conductivity as a function of temperature.

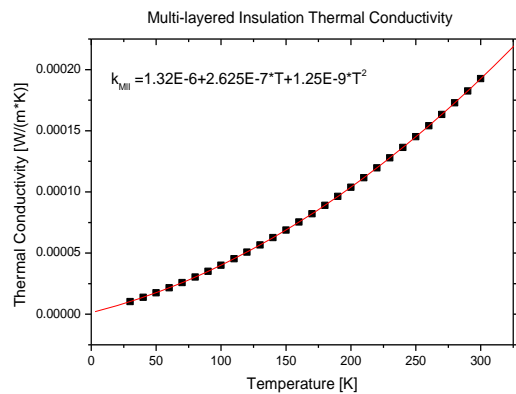


Figure 16. Multi-layered Insulation thermal conductivity as a function of temperature.

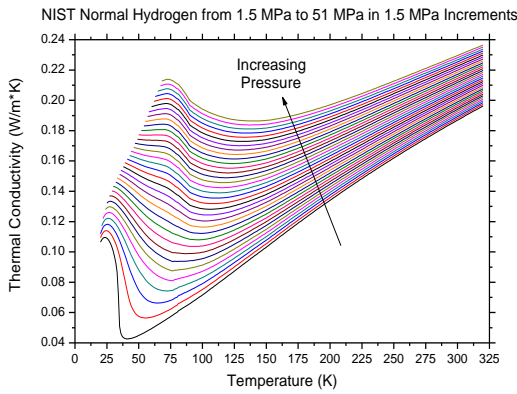


Figure 17. Single phase hydrogen thermal conductivity as a function of pressure and temperature.

As the discharge from the CryoSys Tank into the vacuum volume destroys the multi-layered insulation effectiveness, the thermal conductivity changes as a pure insulating material as shown in Figure 16 to a thermal conductivity described by Figure 10 in the multiphase states for temperatures less than 33 K. For temperatures greater than 33 K, the single phase thermal conductivity given in Figure 17 is incorporated into the analysis.

Since little is known about the discharge coefficient, we have simulated the inside loss of vacuum using three values; namely, 1.0, 0.6, and 0.3. The time-dependent internal CryoSys Tank pressure and average temperature are shown in Figures 18-19, respectively. Note the pressure in Figure 18 when the mechanical safety vent opens.

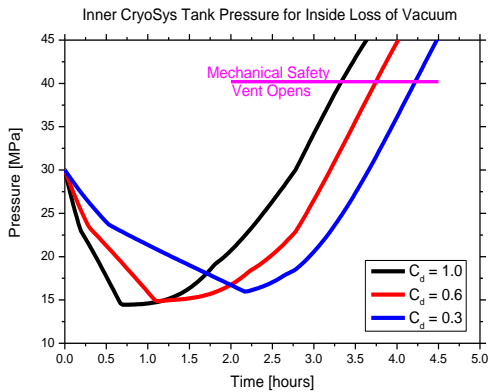


Figure 18. Inner CryoSys Tank pressure during the inside loss of vacuum for three discharge coefficients.

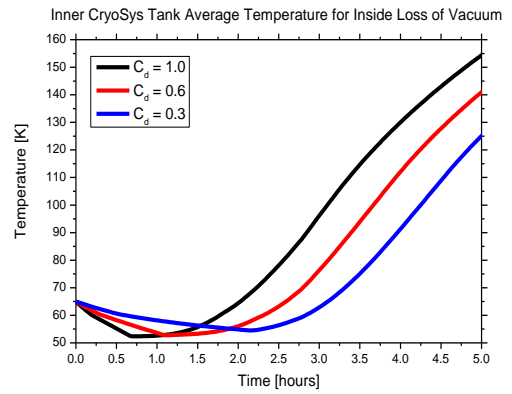


Figure 19. Inner CryoSys Tank average temperature during the inside loss of vacuum for three discharge coefficients.

The initial temperature of the outer Aluminum shell is nearly at the ambient temperature because of the multi-layered insulation’s super-efficiency. During the 5 hour simulation times presented in Figures 18-19, the outer shell is cooled by the very low temperature occurring in the vacuum volume. In Figure 20, we present the outer shell’s average temperature.

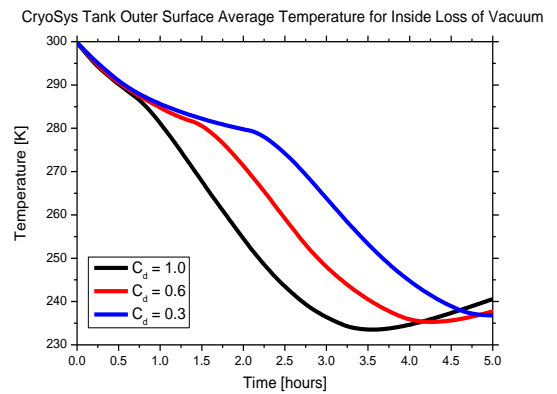


Figure 20. Outer shell average temperature during the inside loss of vacuum for three discharge coefficients.

V. BARE SHELL AND OUTSIDE LOSS OF VACUUM

The time-dependent CryoSys Tank pressures and average tank temperatures for the bare CFE shell and the inside loss of vacuum are presented in Figs. 21 and 22. The exact constant volume heating solution from Section II is seen to be fulfilled in both cases.

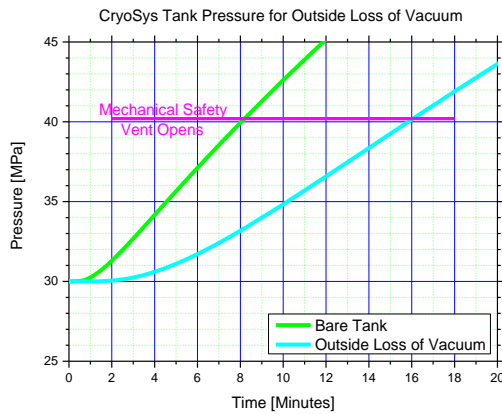


Figure 21. GASFLOW Outside Loss of Vacuum simulation for the CryoSys Tank Pressure.

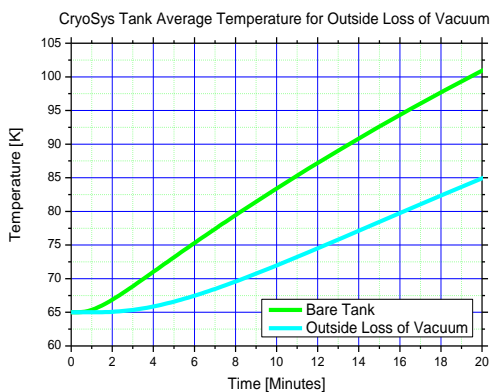


Figure 22. GASFLOW Outside Loss of Vacuum simulation for the CryoSys Tank Average Temperature.

VI. DISCUSSION

As expected, the fastest tank heating case is the bare CFE (steel shell removed) where the CFE surface is exposed directly to ambient conditions. The loss of vacuum from inside, where hydrogen fills the annulus, heats and pressurizes faster than the loss of vacuum from outside, where air fills the annulus.

With the thermal diffusivity for hydrogen being roughly 7 times that of air, the loss of vacuum heating time for the air filled annulus is longest, showing that air is a far better insulator than hydrogen.

The simulations show that the steel shell removed loss of vacuum case heats to within 25 K of the ambient temperature (300 K) in a little more than 5 hours where the inside loss of vacuum (hydrogen filling the annulus) requires nearly double that amount of time (> 10 hours). The outside loss of vacuum (air filling the annulus) then shows about 30 hours to heat within 25 K of the ambient.

ACKNOWLEDGEMENTS

This work was carried out in collaboration with the Institute for Nuclear and Energy Technology (IKET) of the Karlsruhe Institute of Technology (KIT)

REFERENCES

- [1] J.R. Travis, P. Royle, J. Xiao, G.A. Necker, R. Redlinger, J.W. Spore, K.L. Lam, T.L. Wilson, C. Mueller and B.D. Nichols, "GASFLOW: A Computational Fluid Dynamics Code for Gases Aerosols, and Combustion", VOLUME 1, Theory and Computational Model, Karlsruher Institut für Technologie (KIT), Karlsruhe, 2011.
- [2] J.R. Travis et al., "GASFLOW: A Computational Fluid Dynamics Code for Gases, Aerosols, and Combustion", VOLUME 2, User's Manual, Karlsruher Institut für Technologie (KIT), Karlsruhe, 2011.
- [3] P. Royle, J.R. Travis and J. Kim, "GASFLOW -A Computational Fluid Dynamics Code for Gases Aerosols, and Combustion", VOLUME 3, Assessment Manual, Forschungszentrum Karlsruhe GmbH, Karlsruhe, 2008.
- [4] Dr. Kunze / Dr. Kircher, BMW Group, "CRYOSYS-SYSTEMVALIDIERUNG KRYODRUCK-FAHRZEUGTANK.", NIP-VOLLVERS AMMLUNG, BERLIN, 7./8. NOVEMBER, 2011.
- [5] H. Barthélémy, "Hydrogen storage – Industrial perspectives", *Int. J. of Hydrogen Energy*, **37**, 17364-17372, 2012.
- [6] J.R. Travis, J. Xiao, Z. Xu, D. Piccioni Koch and T. Jordan, „Real-gas Equations-of-State for the GASFLOW CFD code“, *Int. J. of Hydrogen Energy*, **38**, 8132-8140, 2013.
- [7] J.R. Travis and D. Piccioni Koch, "GASFLOW Analysis for the HySIM Hydrogen Refueling Benchmark", *Proc. 2nd International Congress on Energy Efficiency and Energy Related Materials (ENEFM2014)*, 16-19 October, 2014, Oludeniz, TURKEY.
- [8] J. Leachman, „Fundamental Equations of State for Parahydrogen, Normal Hydrogen, and Orthohydrogen“, *Masters of Science Thesis*, University of Idaho, 2007.
- [9] J.W. Leachman, R.T. Jacobsen, S.G. Penoncello and E.W. Lemmon, „Fundamental Equations of State for Parahydrogen, Normal Hydrogen, and Orthohydrogen“, *J. Phys. Chem. Ref. Data*, **38**, 721, 2009.
- [10] O. Kircher, (BMW Group), Private communication, February, 2011.
- [11] J.R. Travis, W. Breitung, D. Piccioni Koch and T. Jordan, „A Homogeneous Non-equilibrium Two-phase Critical Flow Model“, *Int. J. of Hydrogen Energy*, **37**, 17373-17379, 2012.
- [12] B. Spang, "Correlations for Convective Heat Transfer", Chemical Engineers' Resource Page. [Online]. Available: www.cheresources.com.
- [13] W.M. Kays and M.E. Crawford, M. E., "Convective Heat and Mass Transfer", McGraw-Hill, 1993.